Acta Crystallographica Section A
Foundations of Crystallography
ISSN 0108-7673

Received 5 March 2003
Accepted 2 October 2003

Topological density of nets: a direct calculation

Jean Guillaume Eon

Instituto de Química, Universidade Federal do Rio de Janeiro, A-631 Cidade Universitária, Ilha do Fundão, Rio de Janeiro, 21945-970 Brazil. Correspondence e-mail: jgeon@iq.ufrj.br

The topological density of a three-dimensional net is currently available after determining its entire coordination sequence. This paper shows that its value can be obtained directly from the set of cycles of the quotient graph of the net. A geometrical tool, the *cycles figure* of the net has been developed for this purpose. Its construction as a convex polyhedron with triangular faces is described as well as its use for topological density calculations. An exact expression is derived for three-dimensional nets and extended to arbitrary n-dimensional nets. Additionally, this paper describes applications to three-dimensional lattices and nets, n-dimensional diamonds and lonsdaleites.

1. Introduction

The topological density (ρ) of a net is a well known numerical invariant proposed for classification and analysis of crystal structures (O'Keeffe, 1991*a*; Bader *et al.*, 1997). This concept was initially defined as the limit for $r \to \infty$ of the local topological density $\rho_r = \sum_{k=1,r} C_k/r^n$, where C_k and n are the kth coordination number and the dimension of the net, respectively. For numerical calculations, however, it was observed that coordination numbers C_k could be written as a periodic set of polynomials of k (Grosse-Kunstleve *et al.*, 1996). One obtains the topological density by averaging the coefficients of degree higher than $(n-1)$ of the kth coordination number and dividing by the dimension n of the net. Determinations of topological densities are thus based on the previous analysis of coordination sequences, usually performed on empirical bases. Recently, the author of this paper developed an algebraic method (Eon, 2002) based on the paths and cycles of the quotient graph of the net to calculate the generating functions for coordination sequences. This work shows that complete knowledge of the generating function is not necessary to calculate the topological density. Instead, it is shown that an exact expression of the topological density of the net is attached to some convex polytope associated with the cycles of its quotient graph.

The fundamental concepts were already discussed in previous papers and are briefly reviewed in §2 in order to make the paper as self-contained as possible. Some of these concepts, however, are presented in a more economical but equivalent way. §3 develops a simple two-dimensional case to introduce the new concept of the *cycles figure* and the method proposed for topological density calculation. The next and central section, §4, gives a formal description of the construction and properties of the cycles figure, including its relation to topological density. The formal demonstration of the relationship is given in Appendix *A* in order to avoid discontinuity of the discussion. §§5–11 provide an analysis of several two- and three-dimensional nets of increasing structural complexity and give evidence of the efficiency of the cycles figure as a practical tool, since the numerical values are already known. The calculation of the topological densities of n-dimensional diamonds and lonsdaleites and the determination of the generating function for the coordination sequence of three-dimensional lattices are proposed as original applications in §§12–15.

2. Theoretical framework

Graph theory (see Harary, 1972) provides the framework to the present analysis of crystal structures and associated nets. The first step is to extract topological information from chemical data. An abstract infinite graph is associated with a crystal structure by mapping atoms to the vertices of the graph and localized bonds between atoms to the edges of the graph. *n-dimensional nets* are thus defined as infinite graphs associated with periodic structures in n-dimensional spaces. Although two- and three-dimensional nets only are chemically meaningful, it has proven valuable to extend the definition to any dimension. It was shown for instance that the frameworks of some structural types such as rock salt, rutile or feldspars can be obtained by orthogonal projection of special embeddings of nets in higher dimensions (Eon, 1998). The *quotient graph* of the net is then defined as the finite graph whose vertices and edges map respectively the classes of translationally equivalent vertices and edges of the net, also called *point lattices* and *line lattices*; the mapping must clearly conserve adjacency relations. In general, we choose to work with the primitive unit cell, in contrast to Blatov (2000), a practice that drastically reduces the size of the quotient graph without loss of information. A positive orientation is arbitrarily chosen for the edges of the quotient graph. Thus, if $e = uv$ is an edge with its positive orientation from vertex u to vertex v, then $-e = vu$ is orientated from vertex v to vertex u. Consider, for example, the square net drawn in Fig. 1(*a*); there is only one vertex per unit cell and two kinds of edges parallel to the principal crystallographic axes linking each vertex to an equivalent neighbor. The quotient graph, shown in Fig. 1(*b*), thus has one vertex and two loops since each edge closes to the unique vertex; each loop can be traversed in both directions, restoring the tetra valence of the vertex. In conformity with the method developed by Chung *et al.* (1984), the loops (a and b) were labeled in Fig. 1(*b*) by crystallographic vectors, which completely defines the net from the quotient graph. It was shown further that the factor group of the space group of the crystal structure by the subgroup of its translations is generally isomorphic to a subgroup of the automorphism group of the quotient graph (Eon, 1998, 1999).

In opposition to previous works, 0-chains and 1-chains of a graph G are defined here as formal linear combinations of vertices and edges, respectively, with integer (positive or negative) coefficients. The *support* of the 1-chain $l = \sum m_i e_i$ is the directed subgraph formed by the edges e_i with non-null coefficients, together with the incident vertices. The positive orientation of the edge in the support is the same as in G if the respective coefficient m_i is positive and opposite otherwise. Two 1-chains are said to be *incompatible* when at least one of the common edges has opposite orientations in the respective supports. The *length* $|l|$ of the 1-chain $l = \sum m_i e_i$ is the total number of combined edges, including repetitions: $|l| = \sum |m_i|$.

The *boundary operator* ∂ is the linear operator mapping 1-chains to 0-chains and defined by $\partial e = v - u$, for $e = uv$. A graph G is said to be *connected* if, for any pair of distinct vertices u and v, there is at least one 1-chain l of G for which $\partial l = v - u$. A *walk* w from u to v is a 1-chain with connected support verifying $\partial l = v - u$. The vertices u and v will also be referred to as the end-points of the walk. A *circuit* is a walk with null boundary ($\partial l = 0$), *i.e.* a closed walk. A 1-chain l is said to *decompose* into a set of (possibly closed) walks w_i if the following conditions hold:

$$l = \sum w_i \quad \text{and} \quad |l| = \sum |w_i|.$$

Decompositions of a 1-chain into itself and possibly the null chain are called *trivial decompositions*.

A *path* is then defined as a walk that cannot contain circuits in any decomposition. Intuitively, the edges of a path are traversed continuously between its two extremities without passing more than once through each vertex. Analogously, a *cycle* is a closed path and can be defined rigorously as a circuit that cannot be decomposed further into smaller circuits, *i.e.* non-trivial decompositions only contain a set of paths. The quotient graph G, being a directed graph, induces an orientation to its paths and cycles; the paths and cycles obtained by reversing the orientation must then be considered as different paths. A g-chain is a 1-chain that can be decomposed into one path at most and a set of cycles. The g-chains of the quotient graph deserve special attention because they map geodesics (shortest paths) between vertices of the associated net. Their set was endowed with a commutative ring structure denoted $\mathbf{Z}[x^G]$ (Eon, 2002).

In $\mathbf{Z}[x^G]$, the sum of g-chains symbolizes the enumeration of the respective geodesics of the net. The product of two g-chains is another g-chain and represents an acceptable decomposition of the latter; more exactly, the product was defined in such a way as to generate a unique geodesic (up to commutativity) to each vertex of the net from the finite set of paths and cycles of the quotient graph. This fundamental result was obtained by introducing zero divisors in the ring. Three properties, namely incompatibility, parallelism and short-cut conditions define zero divisors.

First, the product of two paths as well as the product of two cycles with incompatible support is null by definition. For instance, in the g-chains ring of the quotient graph of the square net, we set

$$x^a x^{-a} = 0,$$

where the exponential notation x^a has been used for the g-chain associated with the cycle a. The second property, parallelism, occurs when some g-chain can decompose into different sets of g-chains. In this case, the products corresponding to all decompositions but one must cancel. The last property is associated with the existence of short-cuts, coming from the presence of topological rings in the net. The product of cycles involved in each ring must be set to zero.

It will be shown in Appendix A that topological density depends exclusively on topological distances in the net between the points of some given point lattice. In consequence, only g-chains originating from the cycles of the quotient graph are relevant to this investigation. In this case, we observe that the three properties, incompatibility, parallelism and short-cuts, can be expressed through what will be called *topological relationships*. These are equalities in the

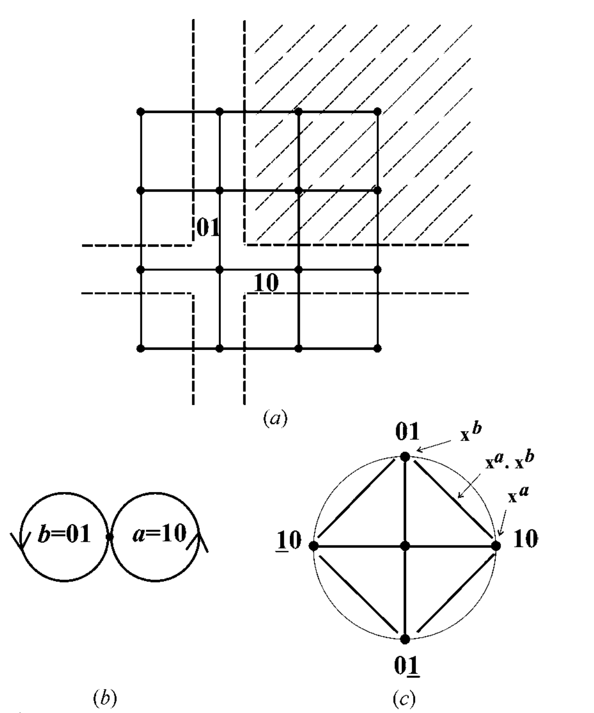

Figure 1
The square-planar net (*a*), its quotient graph (*b*) and its cycles figure (*c*). The regions of the plane in (*a*) have been divided into axes and quadrants by dashed lines parallel to the unit vectors. The hatching marks the region represented by the edge associated with the product $x^a x^b$ in the cycles figure (see text).

case of parallelism or inequalities in the case of incompatibility and short-cuts, arising between the lengths of the cycles of the labeled quotient graph involved in two different decompositions of some g-chain (meaning that the sums of the vector labels are equal in both members of the relationship). We shall use the convention to set to zero the product of g-chains given in the left member. The above incompatibility of opposite cycles of the square net, for example, is a consequence of the topological relationship

$$|a|+|-a|=2>|(0)|=0, \quad \text{with of course } a+(-a)=0.$$

On the other hand, the determination of the generating function for coordination sequences makes use of the cycles part of the generator F (in short, the cycles generator) in the g-chains ring, defined by the formula

$$F\equiv\prod_C\Big(1+\sum_{n>0}x^{nC}\Big),$$

where the product is over all the (oriented) cycles C of the quotient graph. This definition allows the generator to encompass all possible combinations of cycles with repetitions. To deal more easily with infinite sums, it was observed that each factor $(1+\sum_{n>0}x^{nC})$ has the inverse $(1-x^C)$ in the ring, which is easily checked by performing the product. This way, we use preferentially the inverse generator:

$$F^{-1}=\prod_C(1-x^C).$$

The following section is an elementary illustration of these concepts and helps to introduce the graphical method that is developed in this paper as an alternative to calculating the topological density of a net from its quotient graph.

3. Topological density of the square net

Consider again the two-dimensional square net 4^4. First, we determine the inverse generator as defined above:

$$F^{-1}=(1-x^a)(1-x^{-a})(1-x^b)(1-x^{-b}).$$

With the compatibility condition taken into account (the only one defining zero divisors in this net), the inverse generator can be expanded into three terms, combining, respectively, none, one and two loops:

$$\begin{aligned}F^{-1}=1&-(x^a+x^{-a}+x^b+x^{-b})\\&+(x^ax^b+x^{-a}x^b+x^{-a}x^{-b}+x^ax^{-b}).\end{aligned}$$

Hereafter, we will call a product of m factors such as $x^{C1}x^{C2}\ldots x^{Cm}$ a term of order m. F^{-1} is thus comprised of four terms of first order and four terms of second order. At this point, we note that the generator F can be simply derived from its inverse by substituting the infinite sum $S^C\equiv\sum_{n>0}x^{nC}$ for each factor x^C and positive signs for negative ones. This is an immediate consequence of the formal analogy between single factors in the definition of F and their inverse, and can further be verified by direct multiplication. We thus get

$$\begin{aligned}F=1&+(S^a+S^{-a}+S^b+S^{-b})\\&+(S^aS^b+S^{-a}S^b+S^{-a}S^{-b}+S^aS^{-b}).\end{aligned}$$

A graphical interpretation of this expression, based on the definition of the sum in the ring, has been schematized in Fig. 1(a): (i) the first term of F (the constant $1 = x^0$) corresponds to the origin of the lattice; (ii) the second term (combining one loop at a time with all possible repetitions) generates all the vertices of the square lattice localized on the principal axes, each orientation at a time, and excluding the origin; and (iii) the last term (combining two loops at a time) generates all the vertices in the four quadrants of the plane defined by but excluding the a and b axes. For example, the definition of the multiplication and addition laws in the chain ring gives

$$S^aS^b=\Big(\sum_{n>0}x^{na}\Big)\Big(\sum_{n>0}x^{nb}\Big)=\sum_{m,n>0}x^{ma}x^{nb}=\sum_{m,n>0}x^{ma+nb},$$

which stands in F for the enumeration of all the vertices of the lattice inside the first quadrant. As expected, the generator F provides the one-to-one mapping of the vertices of the square net by g-chains of the quotient graph.

Since the relevant information about the whole lattice is already contained in the inverse generator, we take it to define the cycles figure of the net as the polygon (drawn in the plane of the two-dimensional lattice) whose vertices lie at the extremities of the four lattice vectors mapped by the four cycles (loops) of the quotient graph, which appear in the second term of F^{-1} (that is a, b, $-a$ and $-b$); the edges of the cycles figure, by definition, join the vertices corresponding to the loops that are paired in the last term of F^{-1}. The cycles figure, in this case the square shown in Fig. 1(c), is a geometrical representation of the inverse generator. Its vertices describe the terms of first order and its edges the terms of second order. The vertices mapping the two g-chains x^a and x^b and the edge mapping their product x^ax^b have been specifically indicated in the figure. By comparison with the generator F, we observe that the cycles figure provides a triangulation of the sphere S_1, referring to a mapping of all directions and vertices of the plane in the following sense. The edge of the cycles figure corresponding to the term x^ax^b of F^{-1}, for example, stands in F for the product S^aS^b, which enumerates all the vertices of the lattice inside the first quadrant marked by hatching on Fig. 1(a).

The calculation of the generating function G of the coordination sequence is performed by mapping F on the ring of rational functions of the real variable x. Each term S^C must be mapped on the function $x^{|C|}/(1-x^{|C|})$ (Eon, 2002).

$$\begin{aligned}G&=1+4[x/(1-x)]+4[x/(1-x)]^2\\G&=1+4x[1+x+\ldots+x^k+\ldots]\\&\quad+4x^2[1+2x+\ldots+kx^{k-1}+\ldots]\\G&=1+4x+\ldots+4kx^k+\ldots.\end{aligned}$$

After dividing by the dimension of the net, we get $\rho = 2$ ($C_k = 4k$) for the topological density of the square net, as expected. The point is that we do not need the complete expression of the generating function G to get the topological density. The relevant contribution is the coefficient $(4k - 4)$ of x^k coming from the rational function $4[x/(1 - x)]^2$, itself mapping the terms of second order of the inverse generator. This is obviously a consequence of the higher dimensionality of the quadrant in comparison to the lattice axes. It follows that only the higher-dimensional faces (in this case, the edges) of the cycles figure need to be considered in the calculation of the topological density. The next section is devoted to a formal analysis of the properties of the cycles figure and its relations to the cycles generator of the net.

4. Construction and properties of the cycles figure of a net

The mathematical methods formalized in this section present a large analogy to those of algebraic topology, a branch of mathematics that translates topological problems into algebraic ones with the hope they will be solved more easily (Wallace, 1973).

Consider any three-dimensional net with quotient graph G. As mentioned in the second section, the characteristics of the multiplication law in the corresponding chains ring, *i.e.* its zero divisors, must be defined in such a way that the cycles generator provides exactly one g-chain mapping a geodesic from a given vertex to each translationally equivalent vertex of the net. It is not always trivial, however, to formulate unambiguously parallelism and short-cut conditions. The geometrical construction of the cycles figure, considered as a graphical representation of the inverse generator, is proposed to remedy the difficulty. Let us suppose we have already obtained the expansion of the inverse generator in the chains ring. Generalizing the previous two-dimensional example, we describe how a polyhedron can be obtained, its vertices, edges and faces corresponding respectively to the terms of first, second and third order of the inverse generator.

First, the *star* of G in E^3 (the Euclidian three-dimensional space) is defined as the set of lattice vectors mapped by the cycles of the labeled quotient graph (the lattice vectors are given by the sum of the labels along the edges of the cycle of G and will be noted below by the same symbol as the cycle) and drawn from some common origin. The star then maps part of a point lattice. Moreover, it is invariant by the linear constituents of the symmetry operations of the space group of the crystal structure, as proved in Appendix A. However, the symmetry point group of the star is often higher than the crystal class since the two opposite orientations existing for each cycle ensure the presence of a center of symmetry.

Then, points in the direction of the vectors of the star are marked on a sphere drawn from the origin; these points are taken as the vertices of the cycles figure, and represent the terms of first order in the expansion of the inverse generator. Let us say, for example, that the points A, B and C in the directions of the lattice vectors associated with the cycles a, b and c of G represent the terms x^a, x^b and x^c. In simple cases, the end-points of the vectors of the star can be used directly as the vertices of the cycles figure.

Next, we notice that the expansion of the inverse generator cannot contain terms of order higher than three. Indeed, it is not possible to find more than three independent vectors in E^3. Combinations of cycles of higher order should thus cancel in the application of parallelism or short-cut conditions. Besides, it is clear from the calculation given in Appendix B that any term of fourth order, for instance, in the inverse generator would give rise to a coordination number C_k in the form of a polynomial of k of degree three, instead of two for a three-dimensional net. Thus, we can use the terms of third order such as $x^a x^b x^c$ in the expanded inverse generator to define triangular faces (ABC) between the respective vertices (A, B and C) on the sphere. The terms of second order ($x^a x^b$, $x^b x^c$ and $x^a x^c$) corresponding to the three pairs of vertices of the triangle cannot be zero divisors since the ternary product is not null, and so they must be present in the expansion: they define the edges (AB, BC and AC) of the cycles figure. Moreover, a term of third order, such as $x^a x^b x^c$ in the inverse generator leads to a product of the form $S^a S^b S^c$ in the cycles generator. If, as will be observed in general, the matrix of the three lattice vectors a, b and c with respect to the basis vectors of the unit cell is unimodular, then the vector set (a, b, c) can be used as an equivalent basis for the lattice. Consequently, all the vertices of some point lattice of the net in the solid angle limited by the triangular face ABC are enumerated within the product $S^a S^b S^c$; since the role of the cycles generator is to generate exactly once each vertex of the lattice, no superposition of triangular faces is possible. These faces must meet along one of their edges and each edge belongs exactly to two such faces. The procedure leads then to a convex polyhedron providing a complete triangulation of the sphere.

Conversely, a convex polyhedron can naturally be drawn from the star of the quotient graph in many ways. Various conditions must hold in order to identify this polyhedron to the cycles figure of the net. It must be verified that the edges of the polyhedron are not associated with null products in the chains ring and, conversely, that missing edges effectively correspond to zero divisors. Polygonal faces must be triangulated by introducing compatibility, parallelism or short-cut conditions. All this can be done by considering the topological relationships occurring between the cycles of G. If, for each face of the cycles figure, the matrix of the lattice vectors represented by its vertices with respect to the basis vectors of the unit cell is unimodular, then the external surface of the cycles figure can be used to determine the expression of the inverse generator by reversing the procedure described above. Note that the cycles figure is not uniquely determined since parallelism is an arbitrary condition. An exact calculation of the topological density of the net can then be derived as explained in Appendix B. The result is formalized there to avoid discontinuity of the discussion. For n-dimensional nets, each $(n - 1)$-face σ of the cycles figure will be denoted by the n-tuple $(p, q, r, \ldots)$ of the lengths of the cycles mapping its vertices. We define the frequency of a vertex of the cycles figure as the inverse of the length of the cycle mapping the respective vector of the star, and the frequency $f(\sigma)$ of the face σ as the product of the frequencies of its vertices: $f(\sigma)$ =

$(pqr\ldots)^{-1}$. The topological density of the net is proportional to Z, the number of vertices in the quotient graph, and to the sum of the frequencies over its faces: $\rho = Z\{\Sigma_\sigma f(\sigma)\}/n!$. The following sections illustrate the many points of this discussion.

5. The kagome and β-W nets

In this section, we consider two simple plane nets and analyze step by step the construction of their quotient graphs and cycles figures. The kagome net (3.6.3.6) is shown in Fig. 2(*a*); its quotient graph can be obtained and labeled using the general vector method introduced by Chung *et al.* (1984). For this purpose, the vertices and edges of the net have been named within a unit cell chosen as the origin. There are three vertices, namely A, B and C defining three point lattices and six edges, called a to f, defining six line lattices. The three point lattices and six line lattices give rise to the quotient graph K_3^2 represented in Fig. 2(*b*). The vertices of each point lattice are then labeled with the crystallographic vector corresponding to the translation of the translation group from the equivalent vertex inside the origin cell to the respective vertex. The edges are labeled from the difference between the vector labels of their end points. Edge d, for instance, links vertex $B(01)$ to vertex C, *i.e.* $C(00)$, and is labeled (0−1), written (0$\underline{1}$). The resultant labeling of the quotient graph is given in Table 1.

By application of the algebraic method developed in Eon (2002), the generating function of the coordination sequence can be found to be

$$GF(x) = (1 + 4x + 6x^2 + 6x^3 + 3x^4 - 2x^5)/(1 - 2x^2 + x^4).$$

A set of two coordination numbers is then deduced:

$$\begin{aligned} C_k &= 5k - 2, &&\text{for even } k \\ C_k &= 4k + 2, &&\text{for odd } k\ (k > 1),\ C_1 = 4. \end{aligned}$$

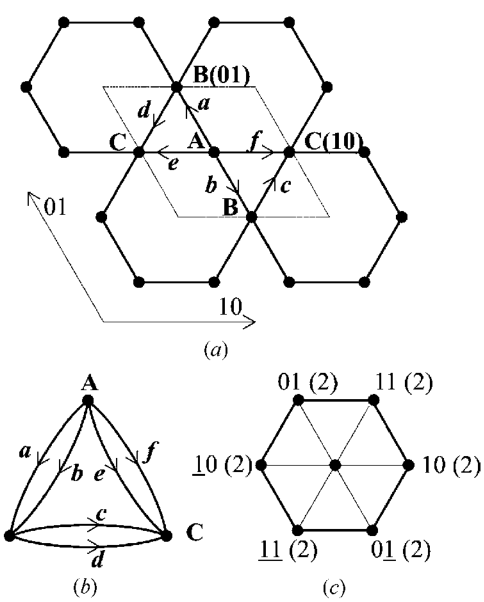

Figure 2
The kagome net (*a*), its quotient graph K_3^2 (*b*) and its cycles figure (*c*).

Table 1
Labeling of K_3^2 for different nets.

	a	b	c	d	e	f
Kagome	01	00	10	0$\underline{1}$	00	10
β-W	0$\underline{1}$	00	00	$\underline{1}$0	00	0$\underline{1}$
Quartz	100	000	011	$\underline{1}$01	010	000

The topological density is the mean value of the linear coefficients of k divided by 2, the dimension of the net: $\rho = 9/4$.

This result can be obtained directly by drawing the cycles figure of the net. By examination of the quotient graph, it is seen that only six different cycles can be obtained, forming the star {10, 11, 01, $\underline{1}$0, $\underline{1}\underline{1}$, 0$\underline{1}$}. The six vertices of this star determine the hexagon shown in Fig. 2(*c*). Conventionally, each vertex of the cycles figure will be labeled hereafter by the mapped cycle, with its length given in parentheses. Note that two cycles of the quotient graph have the same label (11), namely $(a + c - e)$ and $(c - d)$. In this case, only the smaller length in the respective direction must be considered. This amounts to setting $x^{a+c-e} = 0$ in the chains ring, due to short-cut conditions. It is also verified that all products that do not correspond to the sides of the hexagon cancel out by some short-cut condition. Thus, looking at the quotient graph, we see that $x^{f-e}x^{a-b} = 0$, since the cycle $(c - d)$ is a short-cut to the circuit $(f - e + a - b)$ and consequently the cycles figure cannot contain the edge whose end-points are mapped by the two cycles (10) and (01). The same conclusion can be drawn more trivially from the star itself by considering the following topological relationship between its components:

$$|(10)| + |(01)| = 4 > |(11)| = 2,$$
$$\text{with of course } (10) + (01) = (11),$$

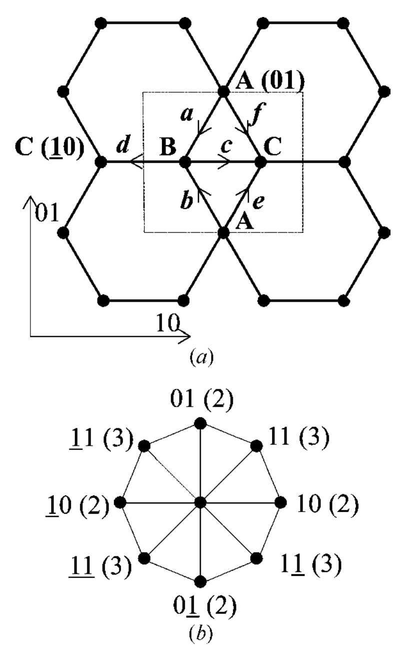

Figure 3
The β-W net (*a*) and its cycles figure (*b*).

where $|(11)|$ is used for the length of the shortest cycle with labeling (11) in the quotient graph.

Since the six 1-faces of the cycles figure are of the type (2,2), the topological density of the kagome net is given by ($Z = 3$):

$$\rho = 3\{6(2.2)^{-1}\}/2! = 9/4.$$

The β-W net is shown in Fig. 3(a). It has the same quotient graph K_3^2 as the kagome net, with its labeling given in Table 1. In this case, the program *TOPOLAN* (Thimm *et al.*, 1994) can be applied to get simply the expression of the coordination numbers.

$$C_k = 4k - 2, \quad \text{for even } k$$
$$C_k = 4k + 2, \quad \text{for odd } k,$$

which gives for the topological density

$$\rho = 2.$$

The star of the quotient graph is constituted by the eight vectors $\{10, 11, 01, \underline{1}1, \underline{1}0, \underline{1}\underline{1}, 0\underline{1}, 1\underline{1}\}$, defining as its cycles figure a non-regular octagon schematized in Fig. 3(b). Short-cut conditions associated with topological relationships clearly hold as, for example, with $|(\underline{1}1)| + |(10)| > |(01)|$. Each 1-face is of the type (2,3), and we verify ($Z = 3$):

$$\rho = 3\{8(2.3)^{-1}\}/2! = 2.$$

6. The (10, 3)-*a* net (O^8)

Let us analyze some three-dimensional nets. The labeled quotient graph, K_4, of the (10,3)-a net (Wells, 1977) is displayed in Fig. 4(a). By convention, null labels are not reported on the graph. The star of K_4 contains three vectors associated with cycles of length 4 (4-cycles): (110), (011) and (101), and four vectors associated with cycles of length 3 (3-cycles): (100), (010), (001) and (111), together with the (seven) opposite cycles. The crystal class is **O**, which leads to point group O_h for the star. As shown in Fig. 4(b), the 3-cycles map the diagonals of the cubic non-primitive unit cell of the net, while the 4-cycles map the directions orthogonal to the faces of the cube, forming a rhombic dodecahedron; the 14 vertices define 12 rhombus faces. However, the product laws defined in the chains ring of the graph K_4 ensure a unique triangulation of this polyhedral surface. Indeed, it is easily verified that (a) in any pair of 4-cycles, the respective supports are not compatible, as for (110) and (101). In the same fashion (b), the only non-null products of 3-cycles arise when these map the boundaries of some edge of the aforementioned cube, as for (100) and (111), but not for (100) and (010), which has the short-cut (110). Again (c), the support of any 4-cycle is compatible with, and only with, the supports of the 3-cycles mapping the vertices of the respective face of the cube, as for (100) and (101), but not for (100) and (011). All these observations can be cast as topological relationships:

(a) $\quad |(110)| + |(101)| > |(100)| + |(111)|,$

(b) $\quad |(100)| + |(010)| > |(110)|,$

(c) $\quad |(100)| + |(011)| > |(111)|.$

Thus, if we draw the edges of the cube, which are associated with a non-null binary product at the surface of the rhombic dodecahedron, we obtain the cycles figure, as is shown in Fig. 4(b). Non-null ternary products are materialized by triangular faces, while products of higher-order systematically cancel.

The cycles figure displays 24 2-faces of the type (4,3,3), which leads to

$$\rho = 4\{24(4.3.3)^{-1}\}/3! = 4/9.$$

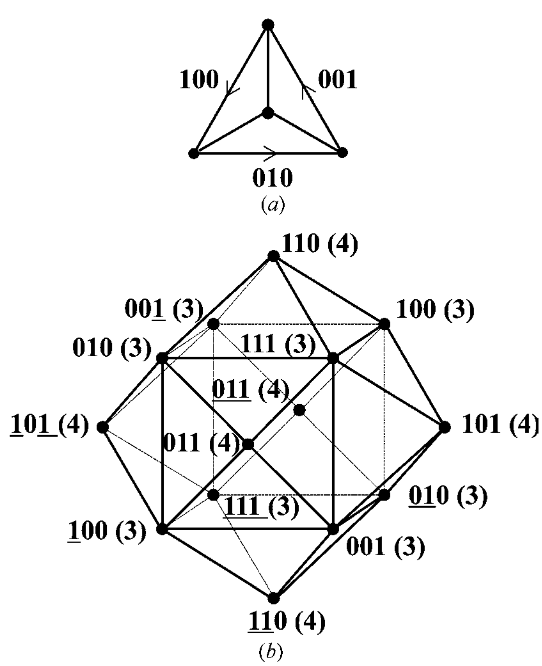

Figure 4
The quotient graph of the (10,3)-a net (a) and its cycles figure (b).

7. The diamond net (O_h^7)

Fig. 5 shows the quotient graph K_2^4 of the diamond net in the primitive rhombohedral cell and its cycles figure. The star of point group O_h contains the six vectors $\{100, 010, 001, \underline{1}10, \underline{1}01, 0\underline{1}1\}$ and the opposite ones, mapping the vertices of a cuboctahedron, all of frequency 2. It is easily checked from the compatibility condition that binary products of cycles cancel if they are not mapped on some common face of the cuboctahedron. The condition is also equivalent to topological relationships, as for instance

$$|(100)| + |(\underline{1}01)| > |(001)|.$$

To achieve the required triangulation, it is necessary to introduce the parallelism condition, canceling out the product between two cycles that map an arbitrary pair of opposite vertices on each square face of the cuboctahedron. Fig. 5(b) illustrates one such possible choice, with for instance

$$|(100)| + |(01\underline{1})| = |(010)| + |(10\underline{1})|.$$

All 20 2-faces of the cycles figure are of the type (2,2,2), giving

$$\rho = 2\{20(2.2.2)^{-1}\}/3! = 5/6.$$

8. The quartz net (D_6^4)

Table 1 gives the labeling of K_3^2 (*cf*. Fig. 2*b*) as the quotient graph of the β-quartz net. The star of point group D_6^h, with 20 vectors, forms the hexagonal prism shown in Fig. 6. The lateral faces of the prism, however, have been cut horizontally into two smaller rectangular faces. Parallelism conditions must be applied to triangulate the hexagonal bases of the prism, as well as the lateral rectangular faces along one of their diagonals. In this case too, it is worth noting that these conditions are equivalently given by topological relationships, such as:

$$|(111)| + |(100)| = |(110)| + |(101)|.$$

We find 12 2-faces of the type (3,3,3) on the hexagonal bases of the prism. On the lateral sides, we count 12 2-faces of the type (3,3,2) and 12 of the type (3,2,2), leading to:

$$\rho = 3[12(3.3.3)^{-1} + 12(3.3.2)^{-1} + 12(3.2.2)^{-1}]/6 = 19/18.$$

However, if O atoms are inserted on the edges, the total number of vertices triples while the length of each cycle doubles. Thus, the correct topological density of the quartz net turns out to be

$$\rho = (3/2^3)(19/18) = 19/48.$$

9. The sodalite net (T_d^1)

The quotient graph of the sodalite net is shown in Fig. 7(*a*). In this case, as for more complex nets, it is hardly possible to obtain the star of the quotient graph by hand; a code has been developed by the author to get the results described below. The triangulation of the sphere was also preferred to the polyhedral representation of the cycles figure to draw the 26 vectors of the star. Based on the cubic symmetry of the star (point group O_h), only one octant of the cycles figure is shown in Fig. 7(*b*). The vectors (110), (101) and (011) correspond to the cubic axes; the direction (111) is along the diagonal of the cube while (211), (121) and (112) are oriented towards the middles of the edges of the cube. Three topological relationships of the same kind lead to the triangulation of the sphere. Thus, for example:

$$|(121)| + |(211)| = 12 > |2(111)| + |(110)| = 10.$$

On the whole sphere, we count 48 2-faces of the type (3,4,6), giving for the topological density (Z = 6)

$$\rho = 6\{48(3.4.6)^{-1}\}/3! = 2/3.$$

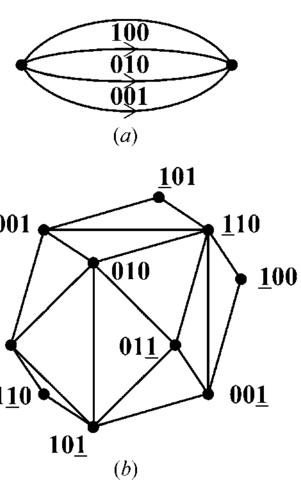

Figure 5
The quotient graph of the diamond net (*a*) and its cycles figure (*b*); the diagonal lines dividing the square faces of the cuboctahedron indicate non-null products based on parallelism considerations (see text).

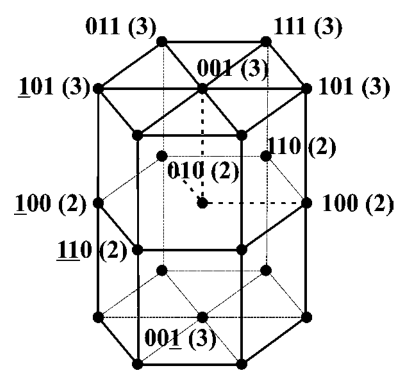

Figure 6
The cycles figure of the quartz net.

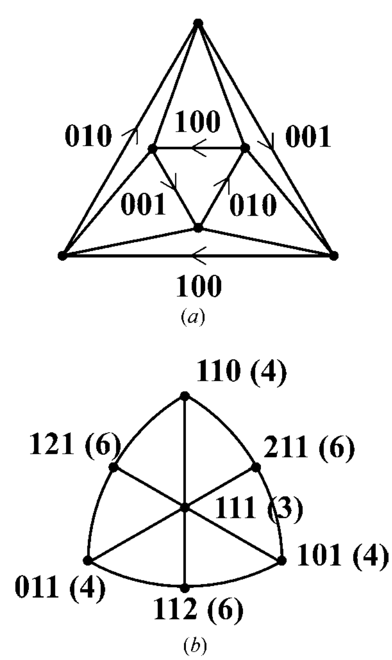

Figure 7
The quotient graph of the sodalite net (*a*) and one octant of its cycles figure (*b*).

10. The cancrinite net (C_6^6)

The quotient graph of cancrinite is shown in Fig. 8(*a*). The hexagonal symmetry (point group C_6^h) of the star limits the discussion to the half superior part of a 60° sector of the cycles figure, shown in Fig. 8(*b*). Two kinds of topological relationship occur:

$$|(102)| > |(101)| + |(001)| \quad \text{(short-cut)},$$
$$|(100)| + |(211)| = |(101)| + |(210)| \quad \text{(parallelism)}.$$

The vertices (102) and (112) have been left in the cycles figure for the sake of completeness although they are set to zero in the chains ring. They have obviously no contribution to the triangulation.

Each of the twelve parts of the cycles figure evidences two 2-faces of type (2,6,10), two of type (6,6,10) and four of type (6,10,10), giving (Z = 12)

$$\rho = 12.12\{2(2.6.10)^{-1} + 2(6.6.10)^{-1} + 4(6.10.10)^{-1}\}/3! = 52/75.$$

11. The orthoclase net (C_{2h}^3)

The quotient graph of the orthoclase net and the superior part ($z > 0$) of the cycles figure are shown in Figs. 9(*a*) and 9(*b*), respectively. The vertices that have no contribution to the triangulation have been left out for the sake of clarity. These are (101), (011), (111), (0$\underline{1}$2) and ($\underline{11}$2). Some of the topological relationships occurring are listed below:

$$|(0\underline{1}2)| = |(011)| + |(001)|$$
$$|(101)| = |(100)| + |(001)|$$
$$|(111)| = |(110)| + |(001)|$$
$$|(1\underline{1}1)| + |(\underline{11}2)| = 13 > |2(0\underline{1}1)| + |(001)| = 11.$$

Many types of 2-faces are present on the whole sphere, namely four of types (3,3,4), (3,3,7), (3,4,4), (3,4,7), (3,6,7), (4,4,5), (4,5,6) and (4,6,7) and eight of type (3,4,6), giving (Z = 8)

$$\rho = 20/27.$$

12. The Z^n lattice nets

Although the cycles figure is a strong geometrical guide that is most useful for two- and three-dimensional nets, the method can still be used in higher dimensions if the nature of the terms of higher order of the cycles generator can be unraveled by combinatorial analysis. The Z^n lattice net is the simplest possible example. Generalizing the square net, the quotient graph of Z^n has one vertex and n loops labeled (1000...), (0100...) *etc.* Since each loop can be traversed in both directions, the star has $2n$ vectors (1000...), ($\underline{1}$000...) *etc.* It is clear that the terms of higher order of the cycles generator must contain each loop, oriented in one or other direction. The number of such products (faces) is thus equal to 2^n, and all faces of the cycles figure are of frequency 1, which gives (Z = 1)

$$\rho = 2^n/n!$$

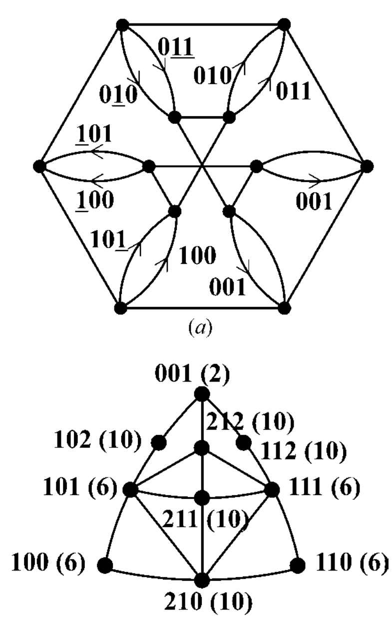

Figure 8
The quotient graph of the cancrinite net (*a*) and a 60° superior sector of its cycles figure (*b*).

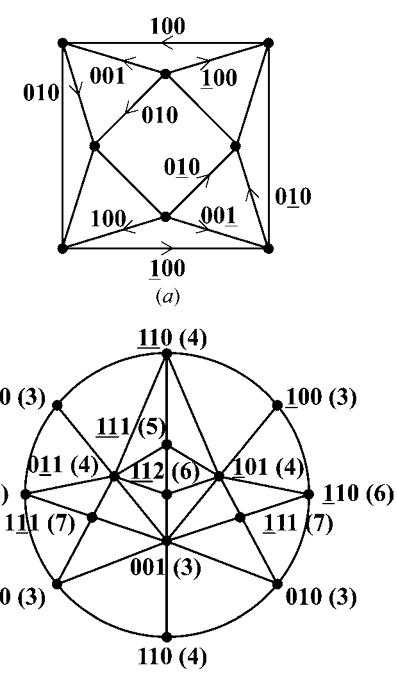

Figure 9
The quotient graph of the orthoclase net (*a*) and the half superior part of its cycles figure.

13. The *n*-dimensional diamond net

O'Keefe (1991*b*) proposed a generalization of the diamond net in higher dimension. The quotient graph has two vertices linked by $n+1$ edges labeled (0000 . . .), (1000 . . .), (0100 . . .) *etc.*, which will be noted $\boldsymbol{i}$ ($i = 1, n+1$) or $\boldsymbol{j}$ ($j = 1, n+1$) when the edge is traversed in the positive or negative orientation, respectively. All cycles have length 2 and the term of higher order of the cycles generator contains n cycles $\boldsymbol{i}_k\boldsymbol{j}_k$ indexed by $k = 1, n$, possibly with repetitions among the edges $\boldsymbol{i}_k$ and $\boldsymbol{j}_k$. Suppose there are p different edges with positive orientation; there are at most $n+1-p$ edges with negative orientation. In fact, the number of edges with negative orientation cannot be inferior to this number. Otherwise, the same product of cycles of order n would be displayed by lower-dimensional diamond nets, meaning that cycles figures in less than n dimensions would present $(n-1)$ faces. Thus, each set of p positive edges determines some $(n-1)$ face of the cycles figure and their number is given by the binomial coefficient C^p_{n+1}.

We now define parallelism relationships ($\approx$) by noting that they originate from exchange of the edges with negative orientation in binary products: $\boldsymbol{i}_1\boldsymbol{j}_2 \cdot \boldsymbol{i}_3\boldsymbol{j}_4 \approx \boldsymbol{i}_1\boldsymbol{j}_4 \cdot \boldsymbol{i}_3\boldsymbol{j}_2$. Thus, we can choose to set to zero the products for which the $\boldsymbol{j}$ sequence is a decreasing function of the $\boldsymbol{i}$ sequence ($1\underline{4}.2\underline{3} = 0$, for example).

The cycles in some product of order n can be ordered by increasing values of the $\boldsymbol{i}$ sequence from left to right. The product can be represented by a set of n boxes (□) separated by $p-1$ walls (|),

$$\square\square\square|\square\square|\square\square\square|\square \ldots \square,$$

where the $\boldsymbol{i}$ values occupy the boxes and are constant between two walls. The $\boldsymbol{j}$ sequence can naturally be ordered by strictly increasing values for constant values of $\boldsymbol{i}$, between two walls. From parallelism relationships, the $\boldsymbol{j}$ sequence is also increasing from left to right. However, it cannot increase after each wall since the total number of $\boldsymbol{j}$ values is exactly $n-(p-1)$. Thus, the position of the walls completely determines the form of the product. The first element on the left corresponds to the smallest $\boldsymbol{i}$ and $\boldsymbol{j}$ values. Between two walls – and before the first wall or after the last one – the $\boldsymbol{i}$ sequence is constant and the $\boldsymbol{j}$ sequence increases; at each wall, the $\boldsymbol{i}$ value increases with the $\boldsymbol{j}$ value remaining constant. The number of such products, which can be interpreted as the triangulation of the $(n-1)$-face, is given by the binomial coefficient $C^{p-1}_{n-1} = C^{n-p}_{n-1}$.

Since all cycles have length 2 (and $Z = 2$), the topological density is given by the following expression:

$$\rho_n = 2\left\{\sum_{p=1,n} C^p_{n+1} C^{n-p}_{n-1}\right\} \Big/ n!2^n = C^n_{2n}/n!2^{n-1}.$$

The last result can be obtained by identifying the coefficient of x^n in the development of the two members of the identity $(1+x)^{2n} = (1+x)^{n+1}(1+x)^{n-1}$. The result is in agreement with the empirical values that were calculated by O'Keeffe (1991*b*) up to $n = 6$.

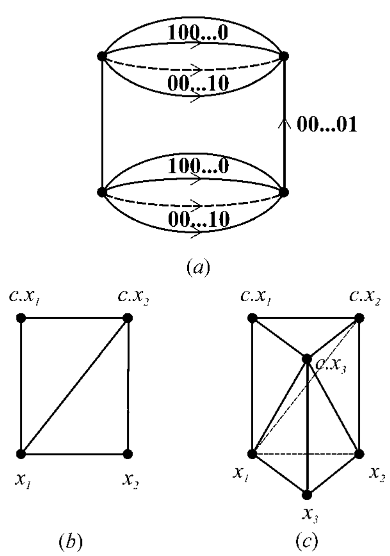

Figure 10
The quotient graph of the n-dimensional lonsdaleite net (*a*), triangulation of the two-dimensional prism (*b*) and the three-dimensional prism (*c*).

14. The *n*-dimensional lonsdaleite net

The generalized n-dimensional lonsdaleite net was also defined in O'Keeffe (1991*b*) as the packing of $(n-1)$-dimensional diamond layers perpendicular to the nth dimension. The quotient graph is formed of two identical copies of the $(n-1)$-dimensional diamond quotient graph linked by two additional edges giving rise to 4-cycles, as shown (vertically) in Fig. 10(*a*). The star contains the vectors $\mathbf{x}_i$ defining the directions inside the layer from the $(n-1)$-dimensional diamond, and their combinations with the nth dimension (c) denoted cx_i and $\underline{c}x_i$ in the following discussion. It is instructive to look first at the cycles figure of the three-dimensional net which corresponds to a double hexagonal prism, as in the case of the quartz net in Fig. 6 (but with different frequencies). This prism can be built by elevation in the third dimension of the two-dimensional cycles figure of the graphite net (two-dimensional diamond), which is the hexagon drawn in the horizontal plane. The argument can be extended to arbitrary dimension and is first discussed in dimension 4. To get the cycles figure of four-dimensional lonsdaleite, a four-dimensional prism (4-prism) has to be drawn by elevation of the cuboctahedron (the cycles figure of diamond) in the 4th dimension. The lateral faces of the 4-prism are themselves 3-prisms, which arise from the elevation of the triangular 2-faces of the cycles figure of diamond. Fig. 10(*c*) shows such a 3-prism based on the 2-face $x_1.x_2.x_3$; the elevated 2-face of this 3-prism is $cx_1.cx_2.cx_3$. Exactly as the rectangular 2-face (2-prism) of the hexagonal prism must be triangulated in three-dimensional lonsdaleite (see Fig. 10*b*), the triangular 3-prism must be triangulated, that is divided into tetrahedral simplexes by introducing new topological relationships between the vertices of their 2-faces. By setting $x_2.cx_1 = x_3.cx_1 = x_3.cx_2 = 0$ in Fig. 10(*c*), for instance, we get the three simplexes: $x_1.cx_1.cx_2.cx_3$, $x_1.x_2.cx_2.cx_3$ and $x_1.x_2.x_3.cx_3$.

The topological relationships can now be formulated in general. Let x_i and x_j be vertices of the star within the $(n-1)$-dimensional diamond layer; they are submitted to the same relationships as described in the previous section. If two such vertices belong to the same face of the cycles figure of the $(n-1)$-dimensional diamond layer, the respective prismatic face of the cycle figure obtained after elevation is triangulated by setting $x_i.cx_j = 0$ whenever $i > j$. Moreover, if $x_i.x_j = 0$, we set $x_i.cx_j = 0$ and $cx_i.cx_j = 0$.

Let $x_1.x_2.x_3 \ldots x_{n-1}$ be some face of the $(n-1)$-dimensional diamond layer: the number of such faces was seen above to be the binomial coefficient C_{2n-2}^{n-1}. The prism based on each such face is then subdivided into the $n-1$ (lateral) simplexes (Wallace, 1973): $x_1.cx_1.cx_2.cx_3 \ldots cx_{n-1}$ (of frequency 2^{1-2n}), $x_1.x_2.cx_2.cx_3 \ldots cx_{n-1}$ (of frequency 2^{2-2n}) $\ldots$, $x_1.x_2.x_3 \ldots x_{n-1}.cx_{n-1}$ (of frequency 2^{n-1-2n}), to which the face in the c (superior) direction, $c.cx_1.cx_2.cx_3 \ldots cx_{n-1}$ (frequency 2^{-2n}), must be added. After equal subdivision on the inferior (c) side, the topological density can be calculated:

$$\rho_n = 8(2^n - 1)C_{2n-2}^{n-1}/n!.2^{2n}.$$

15. Coordination sequences of three-dimensional lattices

The cycles figure can be regarded as a geometrical simplicial complex (Wallace, 1973) providing a polyhedral representation of the product law in the chains ring. In two- and three-dimensional nets, it offers a geometrical support for an immediate calculation of the topological density of the net, but it can also be used as a tool to calculate the complete coordination sequence through its generating function. To illustrate this point, we prove an interesting result proposed by O'Keeffe (1995) for three-dimensional lattices.

In lattices, in contrast to more general nets, all vertices are translationally equivalent, which means that the quotient graph has a unique vertex and multiple loops. Let z be the coordination number of the vertex in the lattice; z is twice the number of loops, and so an even number. Since the star of the quotient graph contains just the loops in both orientations, the cycles figure has exactly $V = z$ vertices. Let F and E be the number of faces and edges of the cycles figure, respectively. After triangulation, every face has three edges, each one being shared by another face, giving $E = 3F/2$. Using the Euler equation ($F - E + V = 2$), we find:

$$E = 3(z-2),$$
$$F = 2(z-2).$$

All loops have length 1 and contain the unique vertex of the quotient graph; no correction for connectedness is needed when mapping the cycles generator to the generating function for the coordination sequence, so that we obtain:

$$\begin{aligned} G(x) &= 1 + V[x/(1-x)] + E[x/(1-x)]^2 + F[x/(1-x)]^3 \\ G(x) &= 1 + zx[1 + x + \ldots + x^k + \ldots] \\ &\quad + 3(z-2)x^2[1 + 2x + \ldots + kx^{k-1} + \ldots] \\ &\quad + 2(z-2)x^3[1 + 3x + \ldots + k(k-1)x^{k-2}/2 + \ldots], \end{aligned}$$

which gives for the kth coordination number:

$$\begin{aligned} C_k &= z + 3(z-2)(k-1) + (z-2)(k-1)(k-2) \\ &= (z-2)k^2 + 2. \end{aligned}$$

A more detailed investigation of cycles figures in general is needed in order to analyze other higher n-dimensional lattices.

APPENDIX *A*
Point symmetry of the star

We begin with the special embedding N of a three-dimensional net obtained by locating the points mapping its vertices at the atomic positions of the crystal structure in E^3, and forming the lines mapping its edges by joining points representing adjacent vertices by straight lines. In this case, the embedding is invariant by the symmetry operations γ of the space group Γ of the crystal, which is then isomorphic to a subgroup of the automorphism group of the net. For simplification, we shall not distinguish between the net and its embedding, nor between the automorphism of the net and the respective symmetry operation of the embedding. Let φ be the mapping of vertices and edges of the net to their class of translationally equivalent vertices and edges, *i.e.* the point and line lattices of the embedding, which constitute the vertices and edges of the quotient graph G. This mapping induces naturally a linear mapping of the chains (0-chains and 1-chains) of the net on the chains of G. It is easy to check that φ commutes with the boundary operators ∂_N in N and ∂_G in G ($\partial_G\varphi = \varphi\partial_N$). We note moreover that the boundary operator also commutes with any automorphism of Γ. Consider now a path V of the net which is mapped by φ on a cycle C of the quotient graph, as schematized in the diagram below.

$$\begin{array}{llll} \varphi: & V \in N & \rightarrow & C \in G \\ & \downarrow \gamma \in \Gamma & & \downarrow a \in \mathrm{Aut}(G) \\ \varphi: & V' \in N & \rightarrow & C' \in G. \end{array}$$

Both end-points of V are then mapped on the same vertex of G, and so belong to the same point lattice in N whereas all other vertices along the path belong to different point lattices. In other words, all the vertices along the path V^* obtained from V by subtraction of its last edge belong to different point lattices. The difference vector in E^3 between the two end-points of the path V is then a lattice vector $\mathbf{S}$ of the embedding associated with a cycle of G, *i.e.* it belongs to the star of G and its Miller indices can be obtained by adding the vector labels of the edges along the cycle C in G (Chung *et al.*, 1984).

A symmetry operation γ of the space group Γ maps the paths V and V^* on equivalent, possibly equal, paths V' and $V^{*\prime}$

of the net, respectively. In particular, all the vertices of $V^{*\prime}$ must belong to different point lattices. It is easy to check that V' is mapped by φ on a cycle C' of G. Indeed, the end-points of V' must belong to the same point lattice since this is the case for the end-points of V. The 1-chain $\varphi(V')$ is thus a circuit of G. If it were not a cycle, it would decompose into at least two smaller circuits of G (by definition of a circuit). But then, the 1-chain $\varphi(V^{*\prime})$ would be equal to the sum of these circuits minus one edge of G, *i.e.* would decompose in at least one circuit. Thus, at least two vertices along $V^{*\prime}$ would belong to the same point lattice, which contradicts the observation made above. This proves that C' is a cycle of G (indeed, φ maps γ on an automorphism a of G, as indicated in the above diagram). Clearly, the difference vector $\mathbf{S}'$ between the end-points of V' belongs to the lattice of the embedding and corresponds to the symmetry transformed of the vector $\mathbf{S}$ by the linear constituent of γ. This shows that $\mathbf{S}'$ belongs to the star of G and completes the proof that the star is invariant by the linear constituents of the symmetry operations of the space group.

APPENDIX *B*
Calculation of topological density

We begin with a useful remark concerning generating functions $G = \sum_k C_k x^k$, where the coordination numbers C_k form a periodic set of quadratic polynomials of k. Consider the product $G' = x^m G = \sum_k C_k x^{k+m}$, where m is any integer such that all $q = k + m$ values are positive. By performing the change $k = q - m$ in the polynomials C_k, these can clearly be written out as a new periodic set C'_q of quadratic polynomials of q, with the same coefficients of degree two, and the same periodicity so that $G' = \sum_q C'_q x^q$. We will refer to this as the asymptotic property of generating functions.

The method proposed here to calculate the topological density of a three-dimensional net is based on the triangulation of the sphere given by the cycles figure of its quotient graph. As shown in §4, any given 2-face representing the product $x^a x^b x^c$ of the inverse generator stands for all the points of some reference-point lattice inscribed within the solid angle defined by the three corresponding vectors of the star $(\mathbf{a}, \mathbf{b}, \mathbf{c})$. The contribution of the reference point lattice to the topological density in this solid angle is determined separately, as shown below, as the coefficient of higher degree of some coordination numbers C_k, written as a periodic set of quadratic polynomials of k. Before doing this, however, we show that all point lattices give an equal contribution to the topological density of the net in the same solid angle. This can be seen by using the path part of the inverse generator (Eon, 2002); the points of any other point lattice are described in the inverse generator by some g-chain of the form $x^p(x^a x^b x^c)$, where p is a shortest path of the quotient graph between the vertices mapping the respective point lattices, and compatible with the three cycles a, b and c. This g-chain introduces a new contribution $x^{|p|} C_k x^k$ in the generating function (with possibly some connectedness correction which can be dealt with in the same way). The result claimed follows immediately from the asymptotic property. In each solid angle, thus, all point lattices contribute the same value to the topological density, which is then proportional to the number Z of vertices contained in the unit cell.

On the other hand, only the triangular faces of the cycles figure need be considered in the determination of the topological density of three-dimensional nets. Indeed, edges and vertices of the cycles figure contribute polynomials of lower degrees to the expression of the coordination number, as the same argument developed below would demonstrate.

Let us look at the contribution of a 2-face associated with three cycles a, b and c of length p, q and r. The product $x^a x^b x^c$ in the cycle generator is mapped on the rational function

$$G = x^\delta [x^p/(1-x^p)][x^q/(1-x^q)][x^r/(1-x^r)],$$

where δ is the (possibly null) correction for connectedness (Eon, 2002).

Let d be the highest common divisor of p, q and r; we write with a prime the corresponding factor, for instance: $p = dp'$. G is then factorized,

$$G = x^{\delta+p+q+r}[1/(1-x^d)]^3[1/(1+x^d+\ldots+x^{p-d})] \times [1/(1+x^d+\ldots+x^{q-d})][1/(1+x^d+\ldots+x^{r-d})]$$

and decomposed into simple elements. The only relevant term (leading to coordination number of degree two) arises from the first, cubic, rational function, since it aggregates the roots of higher multiplicity.

$$G = x^{\delta+p+q+r}[\alpha/(1-x^d)^3] + (\text{terms of lower multiplicity}).$$

The constant α is obtained after multiplication by $(1 - x^d)^3$, then making $x = 1$ in the last two expressions:

$$\alpha = 1/p'q'r'.$$

Now, from multiple derivation of the simple function $1/(1-x)$ relative to the variable x, we get the expansion of the cubic factor:

$$[1/(1-x)]^3 = \sum_k [k(k-1)/2] x^{k-2}$$

or

$$[1/(1-x^d)]^3 = \sum_k [k(k-1)/2] x^{d(k-2)},$$

with the summation index k running over the set of positive integers. We observe that the coefficients of the powers of x are quadratic polynomials of k with trivial periodicity equal to d, since only one among d successive coefficients is different from zero. The same reasoning would show that edges and vertices of the cycles figure contribute linear and constant polynomials of k, respectively, to the coordination numbers.

Considering the periodic set of quadratic polynomials C_k along the period d, the mean value $m(C_k)$ of the coefficient of degree two is independent of the factor $x^{\delta+p+q+r-2d}$, as a consequence of the asymptotic property, and is given by identification:

$$k^2 m(C_k) = [(\alpha/2)(k/d)^2]/d = k^2(2pqr)^{-1}.$$

Taking all the faces of the cycles figure as well as the number Z of vertices of the quotient graph and the dimension (3) of the net into account, the expression for the topological density of three-dimensional nets is finally obtained:

$$\rho = (Z/6)\sum_{\sigma}(pqr)^{-1},$$

where the sum refers to all triangular faces, σ, of the cycles figure.

The above arguments are clearly not restricted to three dimensions and can be generalized to obtain the topological density of n-dimensional nets:

$$\rho = Z\sum_{\sigma}\Big[\prod_{i} p_i^{-1}\Big]\Big/n!,$$

where the sum runs over all $(n-1)$-dimensional faces σ of the cycles figure and the product over the n vertices p_i of the face.

This work was supported by CNPq (Conselho Nacional de Desenvolvimento Científico e Tecnológico) of Brazil.

References

Bader, M., Klee, W. E. & Thimm, G (1997). *Z. Kristallogr.* **212**, 553–558.
Blatov, V. A. (2000). *Acta Cryst.* A**56**, 178–188.
Chung, S. J., Hahn, Th. & Klee, W. E. (1984). *Acta Cryst.* A**40**, 42–50.
Eon, J.-G. (1998). *J. Solid State Chem.* **138**, 55–65.
Eon, J.-G. (1999). *J. Solid State Chem.* **147**, 429–437.
Eon, J.-G. (2002). *Acta Cryst.* A**58**, 47–53.
Grosse-Kunstleve, R. W., Brunner, G. O. & Sloane, N. J. A. (1996). *Acta Cryst.* A**52**, 879–889.
Harary, F. (1972). *Graph Theory.* New York: Addison-Wesley.
O'Keeffe, M. (1991*a*). *Z. Kristallogr.* **196**, 21–37.
O'Keeffe, M. (1991*b*). *Acta Cryst.* A**47**, 748–753.
O'Keeffe, M. (1995). *Z. Kristallogr.* **210**, 905–908.
Thimm, G., Uhr, W., Schumacher, S. & Klee, W. E. (1994). *Z. Kristallogr.* Suppl. 8, p. 595.
Wallace, A. H. (1973). *Introduction à la Topologie Algébrique.* Paris: Gauthier-Villars.
Wells, A. F. (1977). *Three-dimensional Nets and Polyhedra.* New York: Wiley.